

# High spin polarization in all-3d-metallic Heusler compounds: the case of $\text{Fe}_2\text{CrZ}$ and $\text{Co}_2\text{CrZ}$ ( $Z = \text{Sc}, \text{Ti}, \text{V}$ )

Kemal Özdoğan<sup>1</sup>, Igor V Maznichenko<sup>2</sup>, Sergey Ostanin<sup>2</sup>, Ersoy Şaşıoğlu<sup>2</sup>, Arthur Ernst<sup>3,4</sup>, Ingrid Mertig<sup>2</sup> and Iosif Galanakis<sup>5</sup>

<sup>1</sup> Department of Physics, Yildiz Technical University, 34210 İstanbul, Turkey

<sup>2</sup> Institute of Physics, Martin Luther University Halle-Wittenberg, 06099 Halle (Saale), Germany

<sup>3</sup> Institute of Theoretical Physics, Johannes Kepler University, 4040 Linz, Austria

<sup>4</sup> Max Planck Institute of Microstructure Physics, Weinberg 2, 06120 Halle (Saale), Germany

<sup>5</sup> Department of Materials Science, School of Natural Sciences, University of Patras, Patras 26504, Greece

E-mail: [kozdogan@yildiz.edu.tr](mailto:kozdogan@yildiz.edu.tr), [igor.maznichenko@physik.uni-halle.de](mailto:igor.maznichenko@physik.uni-halle.de), [sergey.ostanin@physik.uni-halle.de](mailto:sergey.ostanin@physik.uni-halle.de), [ersoy.sasioglu@physik.uni-halle.de](mailto:ersoy.sasioglu@physik.uni-halle.de) and [galanakis@upatras.gr](mailto:galanakis@upatras.gr)

Received 2 December 2018, revised 5 February 2019

Accepted for publication 18 February 2019

Published 11 March 2019



## Abstract

Employing *ab initio* electronic structure calculations, we study a new class of magnetic Heusler compounds, which consist only of 3d transition metal atoms, namely,  $\text{Fe}_2\text{CrZ}$  and  $\text{Co}_2\text{CrZ}$ , where Z is an early 3d-metal, such as Sc, Ti or V. Although these compounds show a pseudogap and high spin polarization at the Fermi level, the so-called Slater–Pauling rule is not applicable to them.  $\text{Co}_2\text{CrTi}$  and  $\text{Co}_2\text{CrV}$  compounds present robust magnetic properties due to the short range magnetic exchange interactions and, thus, relatively high values of Curie temperature far above the room temperature. Moreover, these two compounds keep their magnetic properties upon B2 disorder that makes them very promising materials for spintronic and magnetoelectronic applications.

Keywords: Heusler compounds, magnetic materials, first-principles calculations, intermetallic compounds

Supplementary material for this article is available [online](#)

(Some figures may appear in colour only in the online journal)

## 1. Introduction

The German metallurgist Heusler, in his search for improving the conducting properties of steel, discovered in the early 20th century a new compound,  $\text{Cu}_2\text{MnAl}$  [1, 2]. During the 20th century it was found, due to the development of instruments, that  $\text{Cu}_2\text{MnAl}$  crystallizes in a cubic f.c.c. lattice, similar to the well-known semiconductors like Si and GaAs, which is also adopted by a large number of intermetallic compounds with a diversity of properties [3, 4]. These intermetallic compounds were named ‘Heusler compounds’ or ‘Heusler alloys’ and several of them are ferromagnetic with high Curie

temperatures [3, 4]. They can be categorized into four distinct families depending on the number and valence of the atoms: (i) the semi-Heusler compounds like  $\text{NiMnSb}$  having the XYZ chemical formula where X and Y are transition metal atoms or lanthanides and Z is a metalloid and their lattice structure is known as  $C1_b$ , (ii) the full-Heusler compounds like  $\text{Co}_2\text{MnSi}$  having the chemical formula  $X_2YZ$  (X, Y and Z atoms are similar to the semi-Heuslers) crystallizing in the  $L2_1$  lattice, (iii) the inverse Heuslers which are similar to the full-Heuslers but the valence of X is smaller than the valence of Y and their lattice structure is known as  $XA$  or  $X\alpha$ , and finally (iv) the ordered quaternary Heusler compounds, like  $(\text{CoFe})\text{TiSi}$

which have the chemical formula  $(XX')YZ$  and crystallize in the so-called LiMgPdSn structure [4, 5]. In all families, Z is a metalloid atom.

The interest in Heusler compounds has been revived in the dawn of the 21st century due to the discovery of half-metallicity which is a common property among several ferromagnetic and ferrimagnetic Heusler compounds [6–9]. Half-metallic compounds present a usual metallic behavior for the majority spin electrons and a semiconducting behavior for the minority spin electrons and thus exhibit high spin polarization at the Fermi level [10]. This property makes them attractive for application in spintronics and magnetoelectronics since they offer new functionalities to devices [11, 12]. Although, also other materials have been explored for their half-metallic properties, Heusler compounds are attractive due to their high Curie temperatures and several studies covering their fundamental properties and their applications have been carried out [13–16]. Recently, some of these magnetic Heusler compounds have been proposed to present even more peculiar behaviors than half-metallicity, such as spin-gapless semiconducting or spin-filtering behaviors, which lead to new functionalities [17].

The simulation of materials using first-principles (also known as *ab initio*) calculations is a powerful tool in order both to understand the properties of the studied compounds as well as to predict new compounds with ‘à la carte’ properties. Extensive databases based on first-principles calculations of hundreds of magnetic Heusler compounds with potential application in spintronics and magnetoelectronics have recently appeared in literature [18–25]. Such databases come to complete the studies focusing mainly on the understanding of the origin of the properties of these compounds, and which thus focus in a small number of Heusler compounds [6–9].

Current growth techniques make possible the growth in the form of films compounds which have been first predicted theoretically. E.g.  $(CrV)TiAl$  a quaternary Heusler compound was predicted in [26] to be a fully-compensated ferrimagnetic semiconductor. Then, it was grown successfully and its unique magnetic properties have been confirmed [27]. In this respect, there is merit in studying new possible Heusler compounds with novel properties. As mentioned previously, in the case of magnetic Heusler compounds, Z is a metalloid, but, already, in the case of Heusler compounds presenting martensitic transformation it has been shown that Z can be fully substituted by a transition metal atom, like  $Mn_2Ni_{1.25}Co_{0.25}Ti_{0.5}$ , and these compounds are called all-3d-metal Heusler alloys or compounds [28–31]. We expand this idea to the case of the magnetic Heusler compounds for spintronics applications, and using first-principles electronic band structure calculations we investigate the properties of all-3d-metal Heusler compounds having the chemical formula  $X_2YZ$  where the valence of the transition metal atoms follows the order  $X > Y > Z$ . All studied compounds were found to be usual magnetic metals. In the present study we focus in the case of  $X_2YZ$  compounds where X is Fe or Co and Z is also an early 3d transition metal element (Sc, Ti or V), since they present a high spin polarization at the Fermi level making them suitable for applications in

spintronics and magnetoelectronics. Our study covers a wide range of properties of these compounds (structural, electronic, magnetic, temperature dependent properties and disorder).

## 2. Computational details

The first part of this study focuses on the zero-temperature ground state properties of the all-3d-metal Heusler compounds. We employed the full-potential nonorthogonal local-orbital minimum-basis band structure scheme (FPLO) to carry out the first-principles electronic band structure calculations [32, 33]. As exchange-correlation potential, we have used the generalized gradient approximation (GGA) [34] which is known to produce accurate results for the half-metallic Heusler compounds with respect to experiment [6, 7]. For all calculations the total energy (in Hartree) has been converged to the 10th decimal point and a dense  $20 \times 20 \times 20$   $\mathbf{k}$ -points grid obeying the Monkhorst–Pack scheme has been used for the integrals in reciprocal space [35].

In order to treat B2-type disorder and doping as well as to calculate the Heisenberg exchange parameters we employ the first-principles Green’s-function method which is based on the multiple-scattering theory [41, 42]. The GGA approximation to the exchange-correlation potential was also used for these calculations [34], as well as a full charge-density treatment to take into account the possible nonsphericity of the crystal potential and the charge density. The maximal angular momentum used was  $l_{max} = 3$  and the integrals over the Brillouin zone were performed using the  $16 \times 16 \times 16$   $\mathbf{k}$ -point mesh. The effect of disorder between the compound sublattices was simulated using the coherent-potential approximation (CPA) [36–38]. The calculation of Heisenberg exchange parameters and magnon dispersion spectra were performed using a denser  $32 \times 32 \times 32$   $\mathbf{k}$ -point grid.

The preferable magnetic ordering in the materials was evaluated using the effective parameters of the magnetic exchange interactions, which may quantify the magnetic ground state. These parameters were obtained using the magnetic force theorem [39] and the total energy is mapped onto the effective Heisenberg Hamiltonian:

$$H = - \sum_{ij} J_{ij} \mathbf{e}_i \cdot \mathbf{e}_j \quad (1)$$

where  $i$  and  $j$  number the magnetic species, and  $\mathbf{e}_i$  is a unit vector in the direction of the magnetic moment of the  $i$ th atom. The critical temperature estimations were obtained using the multi-sublattice mean field (MF) approximation. The technique used here was already successfully applied to some Heusler compounds [40, 49].

## 3. Results and discussion

### 3.1. Structural and electronic properties

As mentioned previously, we have studied the  $Fe_2CrZ$  and  $Co_2CrZ$  compounds where Z is one of the early 3d transition metals Sc, Ti or V. The first step in our study is to determine

**Table 1.** Calculated equilibrium lattice constants  $a_0$  (in Å), atomic and total (per f.u.) spin magnetic moments (in  $\mu_B$ ), spin-polarization at the Fermi level  $P$ , and Curie temperature  $T_C$  (in Kelvin) for the studied compounds. Note that the two Fe(Co) atoms are equivalent in the  $L2_1$  lattice structure.

Compound	$a_0$	$m^{\text{Fe,Co}}$	$m^{\text{Cr}}$	$m^{\text{Sc,Ti,V}}$	$m^{\text{f.u.}}$	$P$	$T_C$
Fe <sub>2</sub> CrSc	5.92	1.057	-0.752	-0.284	1.079	83%	113
Fe <sub>2</sub> CrTi	5.79	1.056	0.486	-0.532	2.074	88%	176
Fe <sub>2</sub> CrV	5.71	1.263	0.787	-0.488	2.824	61%	316
Co <sub>2</sub> CrSc	5.98	0.701	2.252	-0.342	3.312	82%	329
Co <sub>2</sub> CrTi	5.85	1.003	2.435	-0.374	4.067	65%	602
Co <sub>2</sub> CrV	5.76	1.151	2.316	0.222	4.838	71%	679

their equilibrium lattice constant since these compounds have not yet been grown experimentally. Assuming the  $L2_1$  cubic lattice structure we have performed total energy calculations and we have fitted with a third order polynomial curve our results. The minimum of the curve is the calculated (or theoretical as often named) equilibrium lattice constant. The obtained results are presented in the first column of table 1. The calculated values vary between 5.7 and 6 Å close to the values for other magnetic Heusler compounds [7]. As expected, the Co-based compounds present slightly larger lattice constants than the corresponding Fe ones. Also, in the case of early transition metals -Sc, Ti and V- their atomic radius decreases with the increase of their valence since the less-than-half-filled 3d-states become more localized. This is reflected also in the calculated lattice constants and the compounds with Sc have the largest values and the ones with V the smallest with a difference of about 0.2 Å.

At the equilibrium lattice constants, we have performed electronic band structure calculations for all six compounds under study and have extracted the density of states (DOS) per f.u. (formula unit), which is presented in figure 1. The DOS for all six compounds are similar. There is a small DOS intensity low in energy which stems from the  $s$ -states which we do not present in the figures. The obtained DOS is dominated by the 3  $d$ -states of the transition metal atoms, which will be discussed shortly. Due to the large number of 3  $d$ -electrons in the f.u. the presented bands are broad. The majority-spin DOS shows for all six compounds a large intensity around the Fermi level. To elucidate the origin of this peak, we present in figure 2 the atom-resolved DOS for the Co<sub>2</sub>CrTi compound (the situation is similar for all six compounds). The peak at the Fermi level is due to the Cr atom as expected and this has been already observed in other similar compounds like Co<sub>2</sub>CrAl [43]. The Fe and Co atoms have a large number of valence  $d$ -electrons and thus their majority-spin  $d$ -states are almost completely occupied. On the other hand the early transition metal atoms -Sc, Ti and V- have a small number of valence  $d$ -electrons and most of the weight of the corresponding bands is above the Fermi level.

In figure 1 we have also plotted the total DOS per f.u. for the minority-spin electrons. All six compounds present a region of very low DOS around the Fermi level, also known as a pseudogap in the literature. This region is more pronounced in the case of Co-based compounds which make them more attractive for applications with respect to the Fe

based ones. Defects induce states at the borders of the gap and thus wide gaps persist more upon doping. The occurrence of a pseudogap leads to very large values of the spin-polarization,  $P$ , at the Fermi level (defined as the difference between the majority- and minority-spin DOS at the Fermi level divided by their sum). In table 1 we present the values of  $P$  at the Fermi level which is more than 60% in all cases meaning that the majority-spin DOS at the Fermi level is at least four times the minority -spin DOS at the Fermi level. As shown in figure 2, most of the weight of the occupied minority-spin states resides at the Co(Fe) atoms with smaller contributions both from the Cr and the early transition-metal atoms. Both the occupied and unoccupied bands have the same width for all the transition-metal atoms in the unit cell suggesting strong hybridization between the 3d valence orbitals. We will discuss the origin of the pseudogap later.

### 3.2. Magnetic properties

In table 1 we have presented the calculated atomic and total spin magnetic moments for all six compounds under study at their equilibrium lattice constants. In the case of Fe compounds, the Fe atoms present the largest magnitude of the atomic spin magnetic moments. In the case of the Co-based compounds the magnetic behavior differs significantly. The two extra  $d$ -valence electrons offered by the Co atoms to the unit cell now occupy mainly Cr majority-spin states and thus the Cr spin magnetic moments for these compounds are very large approaching the 2.5  $\mu_B$ . With the exception of Fe<sub>2</sub>CrSc compound, which is the compound with the smallest number of valence electrons, in the other cases the Fe(Co) atoms are ferromagnetically coupled to the Cr ones. With the exception of Co<sub>2</sub>CrV, which is the compound with the largest number of valence electrons in the unit cell, the early transition metal atoms -Sc, Ti, V- have spin magnetic moments antiparallel to the Fe(Co) atoms. Each Cr or Z(=Sc,Ti,V) atom is at the center of a cube with Fe(Co) atoms at the corners. Depending on the distance and overlap of the 3  $d$ -wave-functions the coupling between atomic spin magnetic moments can be either ferromagnetic or antiferromagnetic as manifested by the semi-empirical Bethe-Slater rule [44].

The total spin magnetic moment, with the exception of Co<sub>2</sub>CrSc, is close to an integer value being for example almost 4  $\mu_B$  for Co<sub>2</sub>CrTi. This behavior is similar to the behavior of usual half-metallic Heusler compounds crystallizing in the

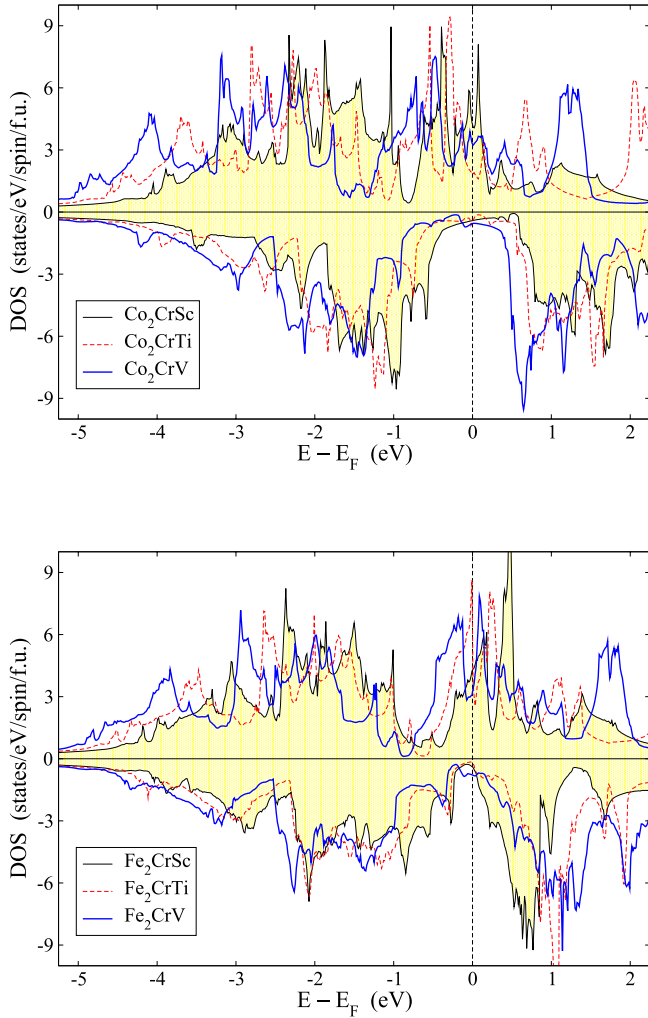


**Figure 1.** Total density of states (DOS) per formula unit for the six studied compounds. The zero in the energy axis is set to be the Fermi level. Positive DOS corresponds to the majority-spin (spin-up) electrons and negative DOS to the minority-spin (spin-down) electrons.

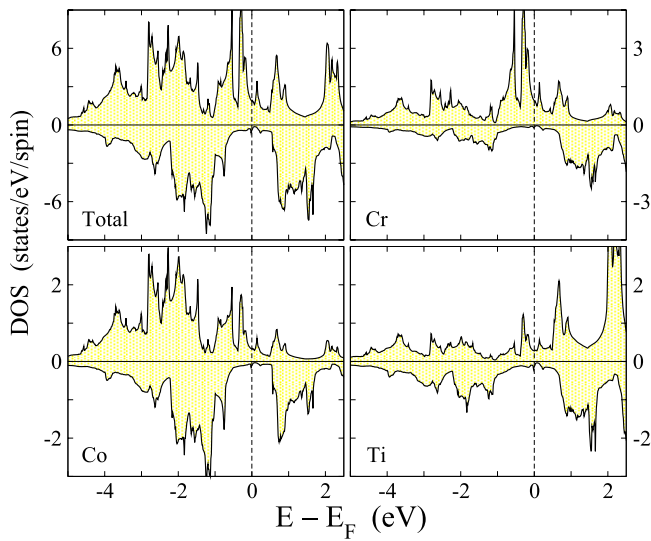


**Figure 2.** Total and atom-resolved DOS for the  $\text{Co}_2\text{CrTi}$  compound. Details as in figure 1.

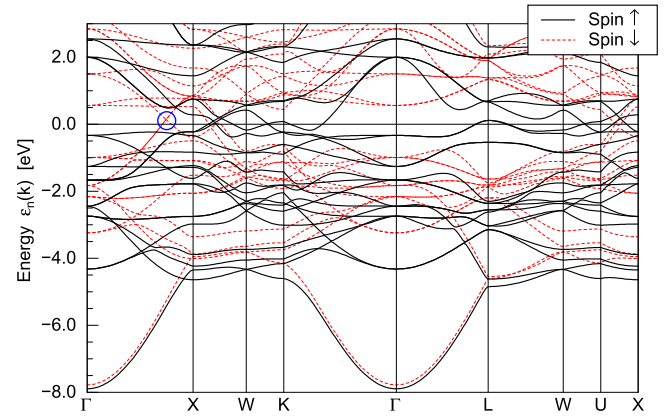


**Figure 3.** Band structure along high-symmetry lines for the  $\text{Co}_2\text{CrTi}$  compound. Note that the band crossing, denoted with a blue circle in the figure, along the  $\Gamma \rightarrow X$  direction between the two minority-spin bands located just above the Fermi level is a Weyl node.

$L2_1$  lattice structure [7]. In the next section we will discuss in detail this behavior investigating its origin.

### 3.3. Origin of the pseudogap

To elucidate the origin of the pseudogap we should perform an analysis similar to the one for other half-metallic Heusler compounds [7]. We will use the  $\text{Co}_2\text{CrTi}$  compounds as the prototype for our discussion. Each Co atom contributes eight valence electrons to the unit cell, Cr 5 and Ti 3, and thus, in total there are 24 valence electrons in the unit cell. Since its total spin magnetic moment is  $4 \mu_B$ , 14 of the 24 electrons are of majority-spin and 10 are of minority-spin character. Therefore, if  $\text{Co}_2\text{CrTi}$  is similar to the usual half-metallic Heusler compounds presenting the Slater–Pauling behavior, there should be exactly ten fully-occupied minority-spin electronic bands. In figure 3 we have plotted  $\text{Co}_2\text{CrTi}$  band structure along several high-symmetry axis and with the red color are the minority-spin bands. The bands exactly at the  $\Gamma$  point are particularly important since their character reveals the character of the corresponding orbitals at the real space from which the bands stem; away from the  $\Gamma$  point the character of the bands changes. First, prior to our discussion, it should be noted that just above the Fermi level there is a band crossing, denoted with a blue circle in figure 3, between two minority-spin bands along the  $\Gamma \rightarrow X$  direction. Calculations using fully-relativistic formalism, similar to the ones in [45], showed that the crossing is invariant under the rotation of magnetization axis and therefore it is a real Weyl node. An extensive discussion of this topological property is beyond the scope of the present article.

In the minority-spin band structure presented in figure 3 at the  $\Gamma$  point there is a single wide band low in energy which is of  $s$  character and stems from the 4  $s$  valence states of all transition metal atoms. This low-energy lying  $s$ -minority-spin band is followed by a large number of 3  $d$ -bands concentrated in a very small energy region between  $-4$  and  $-1$  eV below the Fermi level. In order to characterize these minority-spin

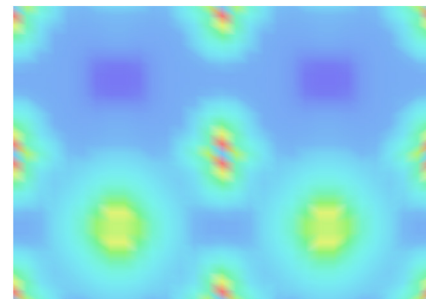
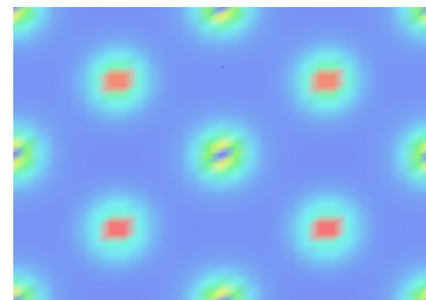
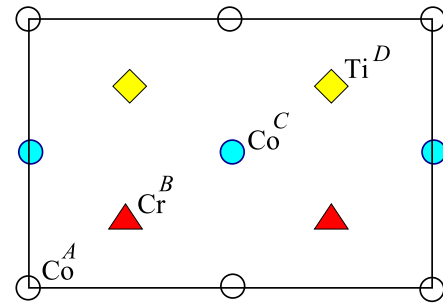
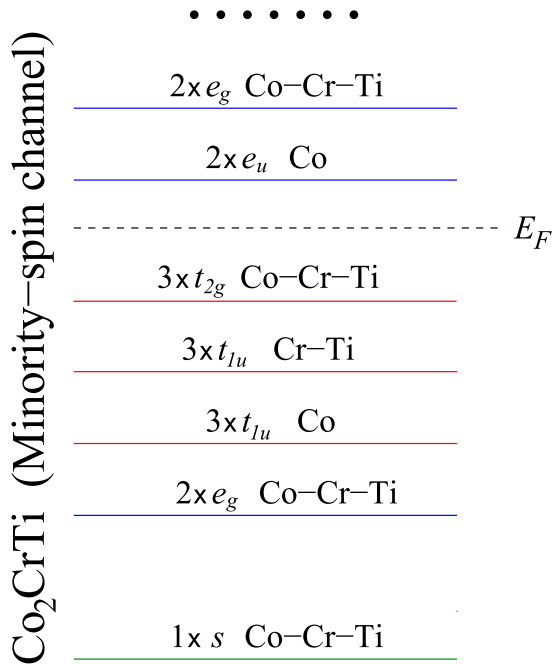


**Figure 4.** Schematic representation of the character of the bands at the  $\Gamma$  point in the minority-spin band structure of  $\text{Co}_2\text{CrTi}$  (see text for details). Note that below the Fermi level there are 12 orbitals which accommodate 10 electrons since the bands away from the  $\Gamma$  point cross the Fermi level and part of their weight is above the Fermi level.

bands we have performed a fat-band analysis similar to the one in [46]. In figure 4 we present schematically the results of our analysis. We denote the degeneracy of the band at the  $\Gamma$  point, the character of the band and the atoms whose orbitals contribute to the band. It should be noted that there are two different types of 3  $d$ -orbitals depending on symmetry similar to the usual full Heusler compounds [7]. The overall symmetry is the tetrahedral one,  $T_h$ . The Co atoms alone form a cubic lattice and thus ‘ungerade’ states obeying only the octahedral symmetry,  $O_h$ , are allowed, which in real space are exclusively localized at the Co atom. The same is true for the cubic lattice formed by the Cr and Ti atoms. First, in energy we meet the lowest lying double degenerate  $e_g$  states which are spread across all atoms. They are followed by the triple-degenerate  $t_{1u}$  states which are localized only at the Co atoms and the triple-degenerate  $t_{1u}$  states which are localized only at the Cr and Ti atoms. Finally, just below the Fermi level there are the triple degenerate at the  $\Gamma$ -point  $t_{2g}$  states which obey the tetrahedral symmetry and to which the 3  $d$ -states of all transition atoms contribute. Thus, in total below the Fermi level there are 12 and not 10 bands as expected if a Slater–Pauling behavior was present in the six compounds under study. These 12 minority-spin bands accommodate in total about ten electrons since away from the  $\Gamma$  point they cross the Fermi level and a substantial part of their weight is above the Fermi level being unoccupied.

To complete our study on the electronic properties of the compounds under consideration we have plotted in figure 5 the distribution of the total charge and total spin densities on the  $(\bar{1}10)$  plane. The spin density is defined as the difference

**Figure 5.** Upper panel: schematic representation of the  $(\bar{1}10)$  plane of the  $\text{Co}_2\text{CrTi}$  compound. Middle panel: distribution of the total charge density for the plane shown in the upper panel; brighter colors correspond to large intensity and deep blue to the almost constant charge density in the interstitial region. Lower panel: distribution of the spin density defined as the charge density for the spin-up electrons minus the charge density for the spin-down electrons; red corresponds to the maximum positive spin density followed by yellow, and dark blue corresponds to the maximum negative spin density.

between the majority-spin and the minority-spin densities. A similar analysis has been made in [46] for the  $\text{Cr}_3\text{Se}$  compounds. The plot of the charge density reveals the fact that Cr and Ti atoms form a cubic lattice on their own. They present similar charge plots which are different from those for the Co atoms. In the case of the spin densities which represent the distribution of the magnetic moment in the space, we can remark

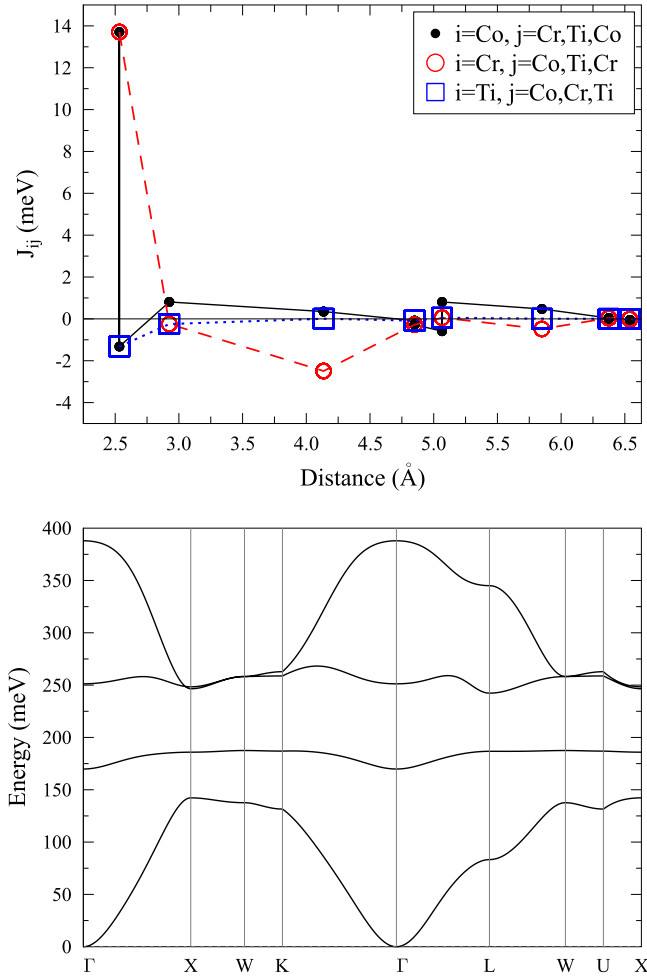


**Figure 6.** Upper panel: exchange constants as a function of the distance in the case of  $\text{Co}_2\text{CrTi}$  compound. See discussion in the text for an extended explanation of the figure. Lower panel: spin-waves dispersion spectrum for the  $\text{Co}_2\text{CrTi}$  compound.

that in the case of Co atoms the spin-density is more localized with a peak (red color) exactly at the center of the atom. On the other hand, in the case of Cr and Ti atoms the spin-density is more delocalized and there is a spherical region around each atom with almost constant spin density. The different color of the Cr (yellow-green) and Ti (blue) spin densities is due to the different sign of their spin magnetic moments.

### 3.4. Exchange constants and Curie temperature

Until now we have discussed the zero-temperature ground-state properties of the considered materials. In the following we focus on the exchange interactions, magnon spectra, Curie temperature, and disorder effects using the KKR code. The calculated Heisenberg exchange parameters as a function of distance for the  $\text{Co}_2\text{CrTi}$  compound are presented in figure 6. Each line with its symbols corresponds to one atom. If two symbols are at the same place this is an intersublattice interaction, while if there is one symbol alone this corresponds to an intrasublattice interaction. We can see that the exchange interactions are dominated by the nearest-neighbor interactions; each Cr or Ti atom has eight Co atoms as nearest neighbors

and each Co atom has four Cr and four Ti atoms as nearest neighbors. First there is a very strong direct ferromagnetic interaction between the Co and the Cr atoms, followed by a weaker Co–Ti direct antiferromagnetic interaction which further stabilizes the magnetic order since Co and Ti atoms have antiparallel atomic spin magnetic moments. The closest Co atoms are next-nearest neighbors and thus, their interaction is weak although ferromagnetic. The nearest Cr–Ti interaction is also indirect since they are next-nearest neighbors and there is a weak antiferromagnetic interaction stabilizing the magnetic order. The only interaction which opposes the magnetic order is the Cr–Cr indirect interaction mediated by the conduction electrons, similar to other Heusler compounds [47], which favors the antiferromagnetic coupling of the Cr spin magnetic moments.

The picture of the exchange constants of  $\text{Co}_2\text{CrTi}$  presented in figure 5 is similar also for  $\text{Co}_2\text{CrV}$ . But the other four compounds show a strongly oscillatory picture. As a result, the magnetic order is not so robust in their case. This behavior is reflected on the calculated Curie temperatures presented in table 1.  $\text{Co}_2\text{CrTi}$  and  $\text{Co}_2\text{CrV}$  present quite high values of the Curie temperature which is 602 K and 679 K, respectively.  $\text{Fe}_2\text{CrV}$  and  $\text{Co}_2\text{CrSc}$ , which have the same number of valence electrons, present Curie temperatures close to the room temperature. The last two compounds  $\text{Fe}_2\text{CrSc}$  and  $\text{Fe}_2\text{CrTi}$  present very low Curie temperatures. Thus, among the six studied compounds  $\text{Co}_2\text{CrTi}$  and  $\text{Co}_2\text{CrV}$  have a merit for applications and in the rest we will concentrate on  $\text{Co}_2\text{CrTi}$  since  $\text{Co}_2\text{CrV}$  present similar behavior.

We have also calculated the magnon (spin-wave) dispersion which is presented in the lower part of figure 5 for  $\text{Co}_2\text{CrTi}$ . There are four branches because there are four magnetic atoms per unit cell. The energy dispersion curve is typical for magnets with short-range interactions, where nearest-neighbor and next-nearest-neighbor interactions dominate. Such interactions do not yield any instabilities; instabilities occur if the acoustic magnon mode (the lowest lying branch) has very low energies (close to zero) in some parts of the Brillouin zone which is not the case here. The acoustic branch of the magnons is well separated in energy from the other three branches and around the  $\Gamma$  point its energy dispersion curve presents a quadratic behavior characteristic of the ferromagnetic and ferrimagnetic materials. This behavior of the magnon dispersion spectrum is similar to other studied ferromagnetic Heusler compounds [48].

### 3.5. Effect of disorder

In the last part of the work we will dwell on the two cases of possible disorder and their effect on the magnetic properties of  $\text{Co}_2\text{CrTi}$  and  $\text{Co}_2\text{CrV}$ . Since both compounds show similar behavior we present the results only for  $\text{Co}_2\text{CrTi}$ . Although the other compounds studied are not promising for applications, we present in the supplementary material, figures S1–S3 ([stacks.iop.org/JPhysD/52/205003/mmedia](https://stacks.iop.org/JPhysD/52/205003/mmedia)) where we have compiled for reasons of completeness our results on all studied compounds.

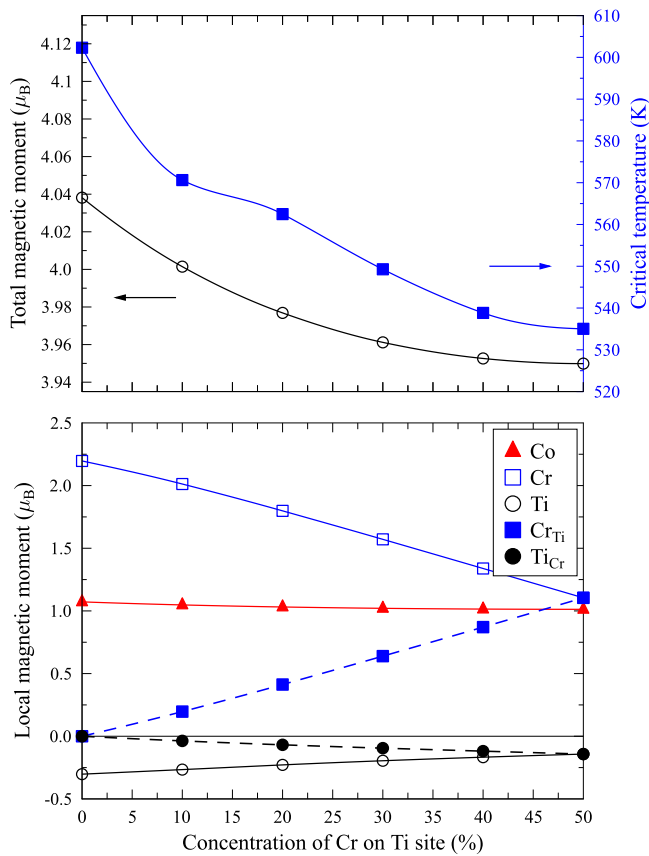


**Figure 7.** Upper panel: variation of the total spin magnetic moment and Curie temperature in the  $\text{Co}_2(\text{Cr}_{1-x}\text{Ti}_x)(\text{Ti}_{1-x}\text{Cr}_x)$  compounds as a function of the concentration  $x$  of the Cr atoms at the Ti sites. The two extremes correspond to the  $L2_1$  and  $B2$  lattice structures. Lower panel: local atomic spin magnetic moments for all atoms in these compounds. Note that the presented values are not scaled to one atom and that lines are just a guide for the eyes.

We consider two cases of disorder. First, we start from  $\text{Co}_2\text{CrTi}$  and we mix Cr and Ti at the two sites keeping the 1:1 stoichiometry of the Cr and Ti atoms in the compounds constant. This models the transition from the fully ordered  $L2_1$  structure to the  $B2$  disordered cases where the Cr and Ti atoms are randomly distributed between the two sites. In figure 7 we present the obtained results as a function of the concentration of Cr atoms at the Ti site. Thus, when the value reaches 50% the two sites are occupied 50% by Cr and 50% by Ti atoms. In the upper panel of the figure we present the behavior of the Curie temperature and of the total spin magnetic moment per unit cell. As we move from the  $L2_1$  lattice to the  $B2$  one, the total spin magnetic moment decreases by only  $0.08 \mu_B$ , and thus, we can safely assume that it remains constant to  $4 \mu_B$  throughout the whole transition. Contrary to the total spin magnetic moment, the Curie temperature shows a more noticeable change, decreasing by about 70 K between the two extremes, although it remains well above room temperature. In the lower panel of figure 7 we present the behavior of the local spin magnetic moments (they have not been scaled to one atom). Interestingly the Co spin magnetic moments remain almost constant throughout the whole transition. This is because they have, for both extremes, the same number of nearest neighbors of each chemical type. In the case of Cr

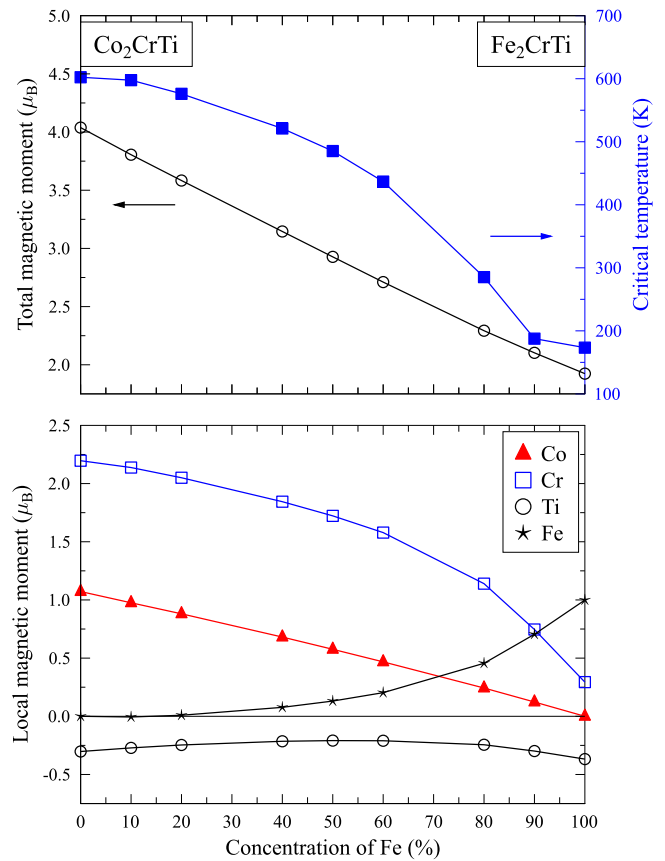


**Figure 8.** Upper panel: variation of the total spin magnetic moment and Curie temperature in the  $(\text{Co}_{1-x}\text{Fe}_x)_2\text{CrTi}$  compounds as a function of the concentration  $x$  of the Fe atoms. The two extremes correspond to the  $\text{Co}_2\text{CrTi}$  and  $\text{Fe}_2\text{CrTi}$  compounds. Lower panel: local atomic spin magnetic moments for all atoms in these compounds. Note that the presented values are not scaled to one atom and that lines are just a guide for the eyes.

atoms, the local spin magnetic moments vary linearly with the concentration. If we scale the local spin moment to one atom, then the linear behavior of the former means that the atomic Cr spin magnetic moment remains constant through the  $L2_1 - B2$  transition. This is also true for the Ti atoms. We can conclude that the Curie temperature is more delicate than the total spin magnetic moment since the disorder may not affect the atomic spin magnetic moments but it affects the exchange constants which determine the Curie temperature. We should finally note that, in experiments, the  $A2$  phase can occur where atoms are randomly distributed to all sites, but such a phase is not interesting for applications in spintronics.

Finally, starting with  $\text{Co}_2\text{CrTi}$  we have investigated the effect of Fe substitution for Co and we present the obtained results in figure 8. The total spin magnetic moment shows a linear decrease between perfect  $\text{Co}_2\text{CrTi}$  and  $\text{Fe}_2\text{CrTi}$  compounds following the behavior of the Co local spin magnetic moment (note that the linear behavior of the Co local spin magnetic moment means that the Co atomic spin magnetic moment is constant throughout the whole transition). The Curie temperature decreases slower than the total spin magnetic moment up to the compound where Fe and Co have equal concentration and it has a value of about 500 K. After that it

decreases very fast reaching the 176 K for Fe<sub>2</sub>CrTi. The local spin magnetic moments follow the behavior of the total spin magnetic moment and of the Curie temperature. The Fe and Cr magnetic moments vary in a non-linear way, contrary to the Co local spin magnetic moment, showing a slow variation at the beginning and then changing quickly.

#### 4. Summary and conclusions

By employing *ab initio* electronic structure calculations we have proposed an alternative class of magnetic Heusler compounds, which consist only of 3d transition metal atoms, with high spin-polarization at the Fermi level. Both families under study Fe<sub>2</sub>CrZ and Co<sub>2</sub>CrZ -where Z is an early transition metal atom Sc, Ti or V- present a region of very low minority spin density of states at the Fermi level while the presence of Cr atom leads to a large majority spin density of states at the Fermi level. Although the total spin magnetic moments per formula unit are close to integer values, a detailed analysis of the minority spin band structure reveals that a Slater–Pauling rule cannot be formulated and there is not an integer number of bands fully-occupied in the minority-spin band structure.

The magnetic state is very stable in the case of the Co<sub>2</sub>CrZ compounds due to the strong short-range interactions and the compounds where Z is Ti or V present high Curie temperatures exceeding 600 K making them candidates for applications. Disorder calculations taking into account the mutual migration of the Cr and Ti(V) atoms show that the resulting B2 structure keeps the characteristics of the fully-ordered L2<sub>1</sub> structure. The substitution of Fe for Co atoms, on the other hand, leads to deteriorated magnetic properties.

Co<sub>2</sub>CrTi and Co<sub>2</sub>CrV compounds exhibit properties which make them ideal potential candidates for spintronic and magnetoelectronic devices. Thus, future experiments are anticipated to grow successfully the proposed compounds.

#### Acknowledgments

This work is supported by the DFG within the Collaborative Research Center *Sonderforschungsbereich* SFB 762. E Ş and IM greatly acknowledge the funding provided by the European Union (EFRE).

#### ORCID iDs

Arthur Ernst  <https://orcid.org/0000-0003-4005-6781>  
Iosif Galanakis  <https://orcid.org/0000-0002-5845-4318>

#### References

- [1] Heusler F 1903 *Verh. Dtsch. Phys. Ges.* **12** 219
- [2] Heusler F and Take E 1912 *Phys. Z.* **13** 897
- [3] Webster P J and Ziebeck K R A 1988 *Alloys and Compounds of d-Elements with Main Group Elements. Part 2 (Landolt-Börnstein, New Series, Group III vol 19)* ed H R J Wijn (Berlin: Springer) pp 75–184
- [4] Ziebeck K R A and Neumann K-U 2001 *Magnetic Properties of Metals (Landolt-Börnstein, New Series, Group III vol 32/c)* ed H R J Wijn (Berlin: Springer) pp 64–414
- [5] Graf T, Felser C and Parkin S S P 2011 *Prog. Solid State Chem.* **39** 1
- [6] Galanakis I, Dederichs P H and Papanikolaou N 2002 *Phys. Rev. B* **66** 134428
- [7] Galanakis I, Dederichs P H and Papanikolaou N 2002 *Phys. Rev. B* **66** 174429
- [8] Skafrouros S, Özdoğan K, Şaşıoğlu E and Galanakis I 2013 *Phys. Rev. B* **87** 024420
- [9] Özdoğan K, Şaşıoğlu E and Galanakis I 2013 *J. Appl. Phys.* **113** 193903
- [10] Katsnelson M I, Irkhin V Yu, Chioncel L, Lichtenstein A I and de Groot R A 2008 *Rev. Mod. Phys.* **80** 315
- [11] Žutić I, Fabian J and Das Sarma S 2004 *Rev. Mod. Phys.* **76** 323
- [12] Hirohata A and Takanashi K 2014 *J. Phys. D: Appl. Phys.* **47** 193001
- [13] Galanakis I and Dederichs P H (ed) 2005 *Half-Metallic Alloys: Fundamentals and Applications (Lectures Notes in Physics vol 676)* (Berlin: Springer)
- [14] Felser C and Fecher G H (ed) 2013 *Spintronics: from Materials to Devices* (Berlin: Springer)
- [15] Fong C Y, Pask J E and Yang L H (ed) 2013 *Half-Metallic Materials and their Properties* (Series on Materials for Engineering vol 2) (London: Imperial College Press)
- [16] Felser C and Hirohata A (ed) 2018 *Heusler Alloys: Properties, Growth, Applications (Springer Series in Materials Science vol 222)* (Berlin: Springer)
- [17] Galanakis I, Özdoğan K and Şaşıoğlu E 2016 *AIP Adv.* **6** 055606
- [18] Gillessen M and Dronskowski R 2009 *J. Comput. Chem.* **30** 1290
- [19] Gillessen M and Dronskowski R 2010 *J. Comput. Chem.* **31** 612
- [20] Ma J, Hegde V I, Munira K, Xie Y, Keshavarz S, Mildebrath D T, Wolverton C, Ghosh A W and Butler W H 2017 *Phys. Rev. B* **95** 024411
- [21] Ma J, He J, Mazumdar D, Munira K, Keshavarz S, Lovorn T, Wolverton C, Ghosh A W and Butler W H 2018 *Phys. Rev. B* **98** 094410
- [22] Sanvito S, Osés C, Xue J, Tiwari A, Zic M, Archer T, Tozman P, Venkatesan M, Coey M and Curtarolo S 2017 *Sci. Adv.* **3** e1602241
- [23] Faleev S V, Ferrante Y, Jeong J, Samant M G, Jones B and Parkin S S P 2017 *Phys. Rev. B* **95** 045140
- [24] Faleev S V, Ferrante Y, Jeong J, Samant M G, Jones B and Parkin S S P 2017 *Phys. Rev. Appl.* **7** 034022
- [25] Faleev S V, Ferrante Y, Jeong J, Samant M G, Jones B and Parkin S S P 2017 *Phys. Rev. Mater.* **1** 024402
- [26] Galanakis I, Özdoğan K and Şaşıoğlu E 2014 *J. Phys.: Condens. Matter* **26** 086003
- [27] Venkateswara Y, Gupta S, Samatham S S, Varma M R, Enamullah, Suresh K G and Alam A 2018 *Phys. Rev. B* **97** 054407
- [28] Ni Z, Guo X, Liu X, Jiao Y, Meng F and Luo H 2019 *J. Alloys Compd.* **775** 427
- [29] Ni Z, Ma Y, Liu X, Luo H, Liu H and Meng F 2018 *J. Magn. Mater.* **451** 721
- [30] Wei Z Y et al 2016 *Appl. Phys. Lett.* **109** 071904
- [31] Wei Z Y, Liu E K, Chen J H, Li Y, Liu G D, Luo H Z, Xi X K, Zhang H W, Wang W H and Wu G H 2015 *Appl. Phys. Lett.* **107** 022406
- [32] Koepernik K and Eschrig H 1999 *Phys. Rev. B* **59** 1743
- [33] Koepernik K Full Potential Local Orbital Minimum Basis Bandstructure Scheme User's Manual ([www.fplo.de/download/doc.pdf](http://www.fplo.de/download/doc.pdf))

- [34] Perdew J P, Burke K and Ernzerhof M 1996 *Phys. Rev. Lett.* **77** 3865
- [35] Monkhorst H J and Pack J D 1976 *Phys. Rev. B* **13** 5188
- [36] Györffy B L 1972 *Phys. Rev. B* **5** 2382
- [37] Györffy B L, Pindor A J, Staunton J, Stocks G M and Winter H 1985 *Phys. Rev. B* **15** 1337
- [38] Oguchi T, Terakura K and Hamada N 1983 *J. Phys. F: Met. Phys.* **13** 145
- [39] Liechtenstein A I, Katsnelson M I, Antropov V P and Gubanov V A 1987 *J. Magn. Magn. Mater.* **67** 65
- [40] Buczek P, Ernst A, Bruno P and Sandratskii L M 2009 *Phys. Rev. Lett.* **102** 247206
- [41] Lüders M, Ernst A, Däne M, Szotek Z, Svane A, Ködderitzsch D, Hergert W, Györffy B L and Temmerman W M 2005 *Phys. Rev. B* **71** 205109
- [42] Geilhufe M, Achilles S, Köbis M A, Arnold M, Mertig I, Hergert M and Ernst A 2015 *J. Phys.: Condens. Matter* **27** 435202
- [43] Galanakis I 2004 *J. Phys.: Condens. Matter* **16** 8007
- [44] Jiles D 1998 *Introduction to Magnetism and Magnetic Materials* (London: Chapman and Hall)
- [45] Chadov S, Wu S-C, Felser C and Galanakis I 2017 *Phys. Rev. B* **96** 024435
- [46] Galanakis I, Özdoğan K and Şaşıoğlu E 2012 *Phys. Rev. B* **86** 134427
- [47] Şaşıoğlu E 2009 *Phys. Rev. B* **79** 100406
- [48] Jakobsson A, Mavropoulos P, Şaşıoğlu E, Blügel S, Ležaić M, Sanyal B and Galanakis I 2015 *Phys. Rev. B* **91** 174439
- [49] Antonov V N, Ernst A, Maznichenko I V, Yaresko A N and Shpak A P 2008 *Phys. Rev. B* **77** 134444